Targetless Scanner Color Calibration*

Gaurav Sharma▲

Digital Imaging Technology Center, Xerox Corporation, Webster, New York

The lack of a scanner calibration target representative of the image medium (substrate and colorants) often limits the accuracy of scanner color calibration. In this paper, a color calibration method is presented for photographic input media that does not require a calibration target. Using characteristic spectral measurements from the image(s) to be scanned, a model for the spectra on the medium is obtained through a principal component analysis. The spectral sensitivity of the scanner provides a model for its operation. By combining the models for the scanner and the medium, the spectral reflectance of the input corresponding to a given set of scanner RGB values can be determined. This provides a spectral calibration for the scanner, which can readily be transformed into a color calibration under any suitable viewing illuminant. Results from simulations and actual calibrations demonstrate the value of the new method.

Journal of Imaging Science and Technology 44: 301–307 (2000)

Introduction

Color calibration of scanners is an important component of system color management. The goal of scanner calibration is to provide a transformation from the scanner measurements (typically, RGB values in three channel scanners) to a device independent color space (such as CIE XYZ space) or to spectral reflectance (from which tristimuli can be readily computed). Most present day color scanners are not colorimetric devices in that they do not satisfy the Luther–Ives[2,3] criterion. Thus, the CIE XYZ color matching functions cannot be expressed as linear combinations of the spectral sensitivity of these devices and a linear calibration transformation matrix cannot be used to transform from scanner RGB to CIE XYZ tristimuli.[4–6] Often, however, very accurate scanner calibration is possible for a single input medium (combination of substrate and colorants) because there are only three degrees of freedom in the spectra of the input medium which are captured through the use of three scanner channels.[7] In order to obtain these precise calibrations, it is also necessary that the calibration transform be represented by general non-linear functions (as opposed to simple matrices) that are capable of representing the complex relation between the scanner RGB values and the colorimetric values.[7] Higher order polynomials, neural networks, and 3-D look-up tables are therefore commonly used for the purpose of scanner calibration.[8]

Typical scanner color calibration is done empirically by scanning a pre-measured calibration target and determining the transformation that maps the scanner RGB values to the measured colorimetric values for the calibration target. The calibration is accurate over the medium represented by the calibration target (i.e., composed of same substrate, same colorants, and same color separation method if there are more than three colorants), but its performance over other media is significantly poorer.

In practice, lack of calibration targets for each scanned medium limits the accuracy of the empirical scanner calibration method. At present, scanner calibration targets are available only from a handful of manufacturers of photoprocessing products.[9] In addition printed images that are to be scanned, need not correspond to the same type and batch of substrate and colorants that were used in the targets.

This article presents a model-based scanner calibration method, which unlike the empirical calibration does not require a calibration target. Instead, the method utilizes models for the medium and the scanner to obtain a calibration transformation. First, from direct measurements or indirect estimation methods spectral models are obtained for the scanner and for the medium of interest. The calibration is then performed by determining for each set of scanner RGB values, a feasible reflectance spectrum for the given medium that would give rise to specified RGB values. The calibration process thus defines a transformation from scanner measurements to spectra (on the given medium) that result in those measurements. The spectra can be readily used to obtain tristimuli under any desired viewing illuminant, which is an additional advantage over schemes that transform scanner measurements into tristimuli under a particular viewing illuminant.

While useful models are clearly not available for arbitrary media, the Beer–Bouger law and Kubelka–Munk theory provide useful models for photographic transparencies and prints, which fortunately constitute a significant fraction of scanned inputs. In this paper, we present a targetless method for calibration for these media.

Original manuscript received March 8, 1999

▲ IS&T Member

* Parts of this paper were presented at IS&T's CIC7.[1]

Spectral Model for Photographic Media

Typical photographic transparencies (and slides) are composed of cyan, magenta, and yellow dyes dispersed in a transparent substrate. Varying the amounts of the three dyes produces different colors required in an image. The dyes and the substrate have negligible scatter and therefore the spectral transmittance of photographic transparencies is well modeled by the Beer–Bouger law.[10] Using the Beer–Bouger law, the transmittance of a sample can be computed from the corresponding dye concentrations as

$$t(\lambda) = t_s(\lambda)\exp\left(-\sum_{i=1}^{3} c_i d_i(\lambda)\right) \tag{1}$$

where λ denotes wavelength, $t_s(\lambda)$ is the transmittance of the substrate, $\{c_i\}_{i=1}^3$ are the concentrations, and $\{d_i(\lambda)\}_{i=1}^3$ the spectral densities of the cyan, magenta, and yellow dyes, respectively, corresponding to unity concentrations. Note that conventionally the logarithm to the base 10 is used in defining density, but for notational simplicity the natural logarithm is used throughout this article. Note also that the concentrations are understood to be normalized relative to the concentrations at which the spectral densities are computed.

Photographic reflection prints are composed of a layer of gelatin in contact with an opaque backing of white paper. Cyan, magenta, and yellow dyes dispersed in the gelatin layer produce colors, with different colors realized, once again, through a variation in the amounts of these dyes. The dye and the gelatin layer have negligible scatter. Therefore, the spectral transmittance of the gelatinous dye-bearing layer can also model by the Beer–Bouger law. The overall spectral reflectance can then be computed by multiplying the square of this transmittance with the reflectance of the backing paper. Alternately, the same result can be obtained from Kubelka–Munk theory[10] (with scattering terms for the colorant set to zero). In either case, the spectral transmittance/reflectance of a print sample can be represented mathematically by

$$r(\lambda) = r_p(\lambda)\exp\left(-\sum_{i=1}^{3} c_i d_i(\lambda)\right) \tag{2}$$

where r_p (λ) is the reflectance (or transmittance) of the substrate, $\{c_i\}_{i=1}^3$ and $\{d_i(\lambda)\}_{i=1}^3$ are the concentrations and *unit concentration* spectral densities of the cyan, magenta, and yellow dyes, respectively. Strictly speaking, a multiplicative factor of 2 is required in the argument of the exponential in Eq. 2 to account for the two-way transmission through the colored layer. This factor is dropped, however, because in what follows, only the mathematical form of these equations is relevant and the factor may be combined with the densities without loss of generality.

Note that Eqs. 1 and 2 are identical in terms of their mathematical form. Only the reflective case of Eq. 2 is therefore be used in further development with the understanding that the case for transparencies may be similarly tackled.

For computational purposes, it is convenient to represent spectra as N-vectors consisting of N uniformly spaced samples over a suitable wavelength interval that covers the spectral region over which the scanner or the eyes are sensitive. Using this sampled representation, Eq. 2 becomes

$$\mathbf{r} = \mathbf{r}_p \otimes \exp(-\mathbf{Dc}) \tag{3}$$

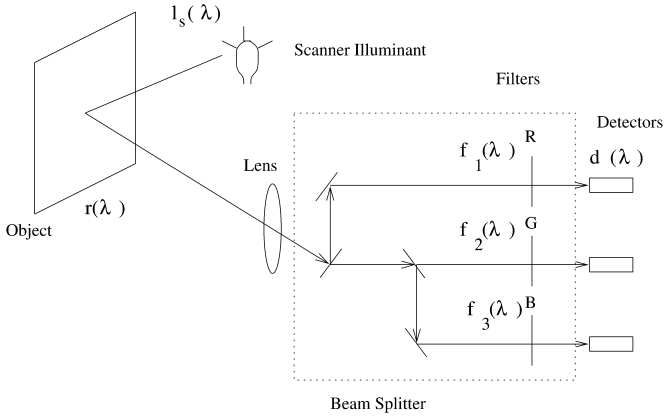

Figure 1. Schematic of a color scanner.

where $\mathbf{r}_p$ is the spectral reflectance of the paper substrate, $\mathbf{D} = [\mathbf{d}_1, \mathbf{d}_2, \mathbf{d}_3]$ is the matrix of colorant densities at unity concentrations, $\mathbf{c}$ is the vector of normalized colorant concentrations corresponding to the reflectance $\mathbf{r}$, ⊗ represents the term by term multiplication operator for N-vectors, and the bold lower case terms represent the spectral N-vectors for the corresponding quantities in Eq. 2.

The model of Eq. 3 provides a means for determining the spectral reflectance of a sample from the concentrations for the cyan, magenta, and yellow dyes. If the range of variation of the concentrations is known, Eq. 3 can be used to determine the set of all reflectance spectra that are producible on the given medium. For example, if the measured dye densities correspond to the maximum concentrations, the set of reflectance spectra producible on the medium can be expressed as

$$S_0^{med} = \{\mathbf{r} = \mathbf{r}_p \otimes \exp(-\mathbf{Dc}) \;\big|\; \mathbf{c} \in \mathbb{R}^3,\ 0 \le c_i \le 1\}. \tag{4}$$

Scanner Model

Figure 1 schematically shows the operation of a typical color scanner. The scanner lamp illuminates the document and the lens onto a beam splitter that splits the light into three channels with red, green, and blue transmitting filter images the light reflected off a small area. The filtered outputs are integrated over the electromagnetic spectrum by optical detectors to obtain a three-band image in red, green and blue channels. For sensors commonly used in electronic scanners, the sensor response is linear and can be modeled as

$$\begin{aligned} t_i &= \int_{-\infty}^{\infty} f_i(\lambda) d(\lambda) r(\lambda) l_s(\lambda) d\lambda \\ &= \int_{-\infty}^{\infty} m_i(\lambda) r(\lambda) d\lambda \qquad i = 1, 2, \ldots 3 \end{aligned} \tag{5}$$

where t_i represents the scanner response for the ith channel, $\{f_i(\lambda)\}_{i=1}^3$ are the spectral transmittances of the color filters (and other optical components), d (λ) is the sensitivity of the detector used in the measurements, $l_s(\lambda)$ is the spectral radiance of the illuminant, $r(\lambda)$ is the spectral reflectance of the pixel being scanned, and $m_i(\lambda) = l_s(\lambda)d(\lambda)f_i(\lambda)$ is the overall spectral sensitivity of the ith scanner channel that incorporates the illuminant spectral irradiant, the detector sensitivity, and the spectral transmittance of the color filter and other optical components. Note that for a variety of reasons[11,6] the scanner RGB responses are often non-linearly trans-

formed on a per-channel basis prior to output. This transformation can however be readily estimated and the model of Eq. 5 can still be used with scanner data with appropriate compensating pre-transformations.

Once again representing the spectral quantities as N-vectors composed of uniformly-spaced samples and approximating the integral by a summation, the scanner model in Eq. 5 can be compactly written in matrix-vector notation as

$$\mathbf{t} = \mathbf{M}^T\mathbf{r} \tag{6}$$

where $\mathbf{t} = [t_1, t_2, t_3]^T$ is the vector of scanner RGB responses, $\mathbf{r}$ is the $N \times 1$ vector of reflectance samples, $\mathbf{M}$ is an $N \times 3$ matrix whose ith column $\mathbf{m}_i$ is the spectral sensitivity of the ith channel, and the superscript T denotes the transpose operation.

Model-based Scanner Calibration

The idea behind model-based scanner calibration is to exploit models for the medium and the scanner to obtain a calibration transformation. The RGB values obtained from the scanner provide information regarding the reflectance spectrum of the pixel scanned. This information is, however, of an incomplete nature because many different (in fact, an infinite number) reflectance, N-vectors can result in the same output triplet of scanner RGB values. The scanner model of Eq. 6 provides a means for better describing the information provided by the scanner RGB values regarding the reflectance spectrum of the input. The reflectance spectrum for a pixel with scanner RGB values given by the vector $\mathbf{t}$ must lie in the set of all possible reflectances that produce the given scanner response $\mathbf{t}$. Using the model of Eq. 6, this set of all possible reflectance's that produce the scanner response $\mathbf{t}$ is mathematically defined as

$$S^{scn}(\mathbf{t}) = \{\mathbf{r} \mid \mathbf{M}^T\mathbf{r} = \mathbf{t}\}. \tag{7}$$

If it is also known that the scanned medium corresponds to the model presented in Eq. 3, the input reflectance lies in the set S_0^{med} of reflectances producible on the medium defined in Eq. 4. Combining the information provided by the scanner RGB values and the scanner model with that for the medium, one can deduce that the reflectance spectrum of the scanned pixel lies in the intersection $S_0^{med} \cap S^{scn}(\mathbf{t})$ of the sets predicated by the scanner model and the model for the medium. For a single photographic medium and typical scanner sensitivities, it is unlikely that "scanner metamers", i.e., different reflectance spectra that appear identical to the scanner will be encountered. (In the presence of "scanner metamers", the notion of what constitutes a valid scanner calibration itself becomes debatable). Therefore, the intersection represents a singleton (one-element) set. In order to illustrate this idea graphically, a synthetic example was created with (1) two samples ($N = 2$) for representing spectra, (2) a medium following Eq. 4 with a single dye with $\mathbf{D} = [0.3, 2.0]^T$, and (3) a single channel scanner with $\mathbf{M} = [0.2, 0.9]^T$. Note the dye and scanner sensitivity correspond to the common situation in which the dye's absorption maximum corresponds to the scanner sensitivity peak. This example is shown in Fig. 2. The two axes of the graph represent samples of the "reflectance" spectrum at the two wavelengths. The set of feasible spectra on the given medium is shown by the solid curve in Fig. 2. The scanner response corresponding to a given dye concentration (0.3) was computed and the set of all spectra

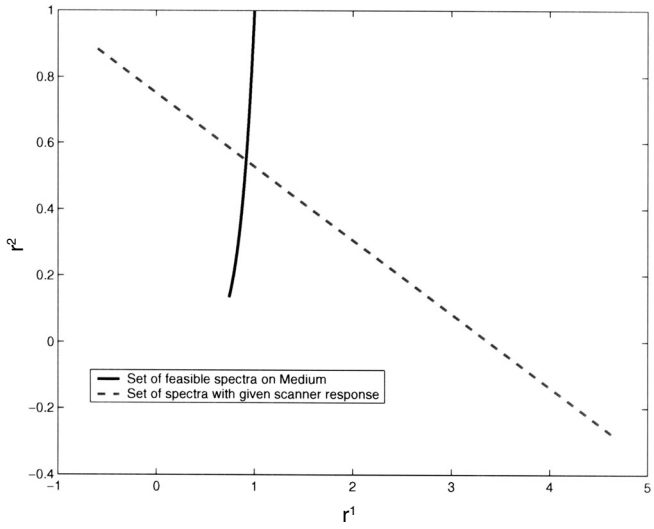

Figure 2. Synthetic two-dimensional example illustrating model-based scanner calibration.

that result in this given scanner response was computed. The broken straight line in Fig. 2 shows this set. Note that while there are several spectra that can produce the given scanner response, only one of these lies in the set of feasible spectra on the given medium and this spectrum is the point of intersection of the solid curve and the broken line in Fig. 2.

From the above description, it is clear that the input reflectance spectrum can be estimated if an algorithm is available for obtaining a reflectance in the intersection of the sets S_0^{med} and $S^{scn}(\mathbf{t})$. Set-theoretic estimation methods[12] specifically address the problem of determining an element in the intersection of a number of constraint sets. The most powerful and useful set-theoretic estimation algorithms are variants of the method of successive projections onto convex sets (POCS),[12] which determines an element lying in the intersection of a number of closed-convex sets by starting with an arbitrary point and successively projecting onto the sets till convergence is achieved.

The set $S^{scn}(\mathbf{t})$ is a closed convex set (under the normal Hilbert space[13] structure on $\mathbb{R}^N$) but the set S_0^{med} is not a convex set (in the same Hilbert space). Therefore, the POCS method cannot be directly applied to the model-based scanner calibration problem. Note, however, that the set S_0^{med} is closed and convex in the density domain. The problem can therefore be formulated in the generalized product space framework proposed recently in Ref. 14. By introducing a suitable Hilbert space structure over the space of reflectance spectra that makes the set S_0^{med} convex, the POCS algorithm can be used. Only the final algorithm for the model based scanner-calibration shall be described here, details of the derivation using the generalized product space framework mentioned above can be found in Ref. 15, where application of the product space formulation to other problems in color science is also described.

Practical Implementation

To implement the model-based scanner calibration method in practice, the models for the scanner and the medium need to be known. The scanner model is defined solely by its spectral sensitivities, which may be determined either by direct measurement or through

an estimation using independent targets.[16] If data for the substrate and dyes is available from the manufacturer, the model of the medium can be obtained from that data. However, in order for the method to be really useful, the medium model needs to be derived directly from the image(s) to be scanned.

Because pure cyan, magenta and yellow tone prints are not normally available in images, the densities corresponding to the dyes cannot be directly measured. Note, however, that by taking the natural logarithm the spectra in the model of Eq. 3 can be rewritten in terms of density as

$$\ln(\mathbf{r}_p) - \ln(\mathbf{r}) = \mathbf{Dc} = \sum_{i=1}^{3} c_i \mathbf{d}_i \tag{8}$$

The left-hand side in the above equation represents the density corresponding to the reflectance $\mathbf{r}$ relative to the white paper reflectance $\mathbf{r}_p$. From the above equation, it is clear that these paper-relative spectral densities are linear combinations of the three dye densities $\{\mathbf{d}_i\}_{i=1}^{3}$. Hence, the paper-relative spectral densities lie in a three dimensional subspace of the overall N-dimensional space containing the spectral density vectors (excluding noise effects). Principal components analysis (PCA)[17] provides a means for determining a set of basis vectors for this three dimensional space.

PCA of an ensemble of paper-relative densities computed from a set of representative spectra in accordance with the left hand side of Eq. 8 yields three significant principal components that explain almost the entire variation in the data.[18] These three significant principal components, referred to as *principal dye densities*,[19] form an orthonormal basis set for the three dimensional space in which paper-relative densities lie. Though the principal components do not correspond to actual dye densities, they span the same subspace as the actual dye densities, i.e., any vector that is expressible as a linear combination of three dye densities can also be expressed as a linear combination of the three principal components, and vice versa. Thus, if the actual densities corresponding to the dyes are not known, the principal dye densities determined from PCA can be used in the model of Eq. 4 instead of the actual densities.[18,19] While the concentrations corresponding to the real dye densities in Eq. 4 were subject to simple upper and lower bounds, similar bounds cannot be obtained for "concentrations" corresponding to the virtual dyes obtained from the principal components analysis. The information in the bounds is therefore lost in this method.

The "principal dye" densities can be determined from a small number of spectral measurements on the scanned images themselves and therefore do not require a calibration target. If $\mathbf{O} = [\mathbf{o}_1, \mathbf{o}_2, \mathbf{o}_3]$ is the matrix of the (orthogonal) principal dye densities (obtained through the principal components analysis), the constraint set

$$S^{med} = \{\mathbf{r} = \mathbf{r}_p \otimes \exp(-\mathbf{Oc}) \mid \mathbf{c} \in \mathbb{R}^3\} \tag{9}$$

can be used to describe producible spectra on the given medium (strictly speaking, this set is a super-set of the producible spectra).

The model for the medium can be then used along with the scanner model to obtain a calibration. Corresponding to each scanner measurement $\mathbf{t}$, a spectral reflectance estimate $\hat{\mathbf{r}}$ is obtained by computing a feasible spectrum lying in the constraint sets S^{med} and $S^{scn}(\mathbf{t})$.

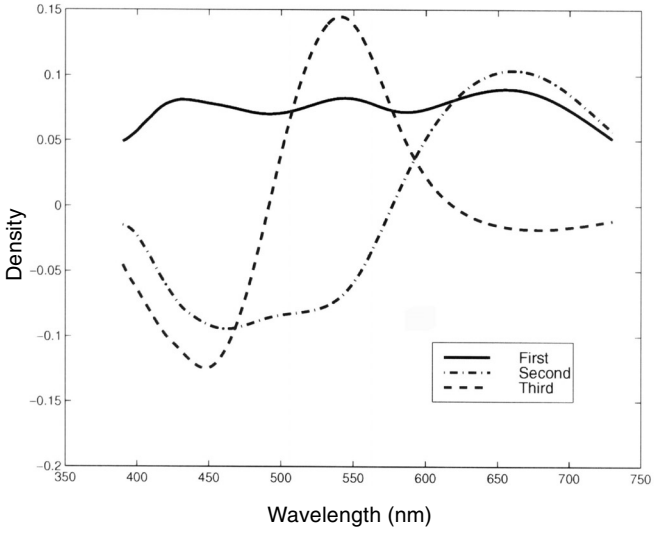

Figure 3. Principal Dye Densities for the Kodak IT8 photographic target.

An outline of the complete algorithm used for this estimation is given in Table I. Note that the averaging step of Eq. 5 in the algorithm is a computational simplification of the true POCS algorithm. Unlike conventional methods of empirical scanner calibration, which transform the scanner RGB values into colorimetric values under a specified viewing illuminant, the method presented here provides a means for recovering complete spectral information, thereby overcoming potential problems due to metamerism. One may note here that an alternate model-based scanner calibration method was proposed in Ref. 20, where, however, the dye densities were obtained directly from manufacturer specifications and a direct optimization approach was used instead of the algorithm presented here. For the non-physical principal dyes obtained from the PCA analysis described earlier, the algorithm of Table I was found to be more robust and less prone to convergence problems than the direct optimization approach.

The results of applying this model-based scanner calibration method to a simulated scanner and to an actual scanner are described in the next two sections. In both cases, the Kodak IT8 photographic target[9] is used for testing the model-based calibration scheme. The reflectance spectra for the 264 patches in the Kodak IT8 target were measured independently using a spectrophotometer. The reflectance of the white patch in the gray-wedge on the target is used as the reflectance of the paper substrate $\mathbf{r}_p$ in computing paper-relative spectral densities. The first three principal components of the 264 densities account for 97.2% of the signal energy in density space, and are used as the (orthonormal) densities $\mathbf{o}_1$, $\mathbf{o}_2$, $\mathbf{o}_3$ of three principal dyes constituting the prints. These principal dye densities are shown in Fig. 3.

Simulation Results

A three-channel color scanner is "synthesized" by defining sensitivities for its channels as the combination of the Wratten[21] WR-26 red, WR-49 green, and WR-52 blue filters with a cool white fluorescent lamp (the scanning illuminant). The resulting scanner sensitivities for the three channels are shown in Fig. 4. In order to test the model-based calibration scheme, scanner RGB val-

TABLE I. Algorithm for Model-Based Scanner Calibration.

1. Set **M** as the spectral sensitivity of the scanner, $\mathbf{r}_p$ as the white paper reflectance of the scanned medium, **O** as the matrix of orthonormal principal dye densities for the scanned medium, and **t** as the set of scanner RGB values for which a calibration is desired.
2. Initialize $i = 0$; and spectral estimate $\mathbf{r}_i = (\mathbf{M}^T)^\dagger \mathbf{t}$, where † indicates the pseudo-inverse. Set components of $\mathbf{r}_i$ that are zero or negative to a small positive value and values above unity to 1.
3. Determine nearest point in $S^{scn}(\mathbf{t})$ the set of spectra that produce the given scanner measurement
$$\mathbf{x} = (\mathbf{M}^T)^\dagger \mathbf{t} + (\mathbf{I} - (\mathbf{M}^T)^\dagger (\mathbf{M}^T))\, \mathbf{r}_i)$$
4. Determine "nearest point" in S^{med} the set of spectra that can be produced on the given medium (using appropriate distance metric)
$$\mathbf{y} = \exp(\ln(\mathbf{r}_p) - \mathbf{O}\mathbf{O}^T(\ln(\mathbf{r}_p) - \ln(\mathbf{r}_i)))$$
5. Obtain next estimate of reflectance by averaging the points in the two sets
$$\mathbf{r}_{i+1} = (\mathbf{x} + \mathbf{y})/2$$
Set components of $\mathbf{r}_{i+1}$ that are zero or negative to a small positive value.
6. Update iteration count: $i = i + 1$
7. Check for convergence: If $\mathbf{r}_i$ is not in $S^{med} \cap S^{scn}(\mathbf{t})$ return to step 3 otherwise proceed to step 8.
8. Set $= \mathbf{r}_i$. This is the estimate of the reflectance on the given medium corresponding to the scanner measurement **t**.

ues **t** are generated using the model of Eq. 6 and the measured reflectance **r** for each patch on the Kodak IT8 target. A spectral reflectance estimate $\hat{\mathbf{r}}$ corresponding to the scanner measurement **t** is then obtained using the algorithm of Table I. Typical results obtained from this procedure are shown in Fig. 5, where the measured reflectance corresponding to a number of the Kodak IT8 patches are shown by the solid lines and the corresponding estimates of spectra obtained from the above procedure are shown by the broken lines. In each case, the broken line closest to a solid line represents the corresponding estimate. Note that in all cases the estimates are quite close to the measured spectra and the error in the calibration is therefore quite small.

In order to quantify the accuracy of the model-based calibration scheme, the computed spectrum $\hat{\mathbf{r}}$ is compared with the actual spectrum **r** using three different metrics:

1) the normalized mean squared spectral error (NMSSE) defined (in dB) as
$$\text{NMSSE} = 10 \log_{10} \left(\frac{E\left\{ \|\mathbf{r} - \hat{\mathbf{r}}\|^2 \right\}}{E\left\{ \|\mathbf{r}\|^2 \right\}} \right), \qquad (10)$$
where $E\{\bullet\}$ denotes the average over the spectral ensemble (in this case the Kodak IT8 target spectra),

2) the ΔE^*_{ab} color-difference[22] under CIE D50 daylight illuminant, and
3) the ΔE^*_{94} color-difference[23] under CIE D50 daylight illuminant.

The NMSSE measures the spectral error in the calibration and the ΔE metrics attempt to quantify the visual impact of the spectral errors.

For the simulated model-based scanner calibration described above, the NMSSE is –33.84 dB and the ΔE^*_{ab} error has an average value of 0.62 and a maximum value of 2.59 over the 264 patches in the Kodak IT8 target. The corresponding average and maximum numbers for the ΔE^*_{94} metric are 0.32 and 0.93, respectively. The small magnitude of NMSSE indicates that the model-based scanner calibration approach is successful in providing a spectral calibration. The color errors represented by the ΔE^*_{ab} and ΔE^*_{94} statistics are also quite small and comparable to or better than the accuracy typically obtained for scanner calibration.

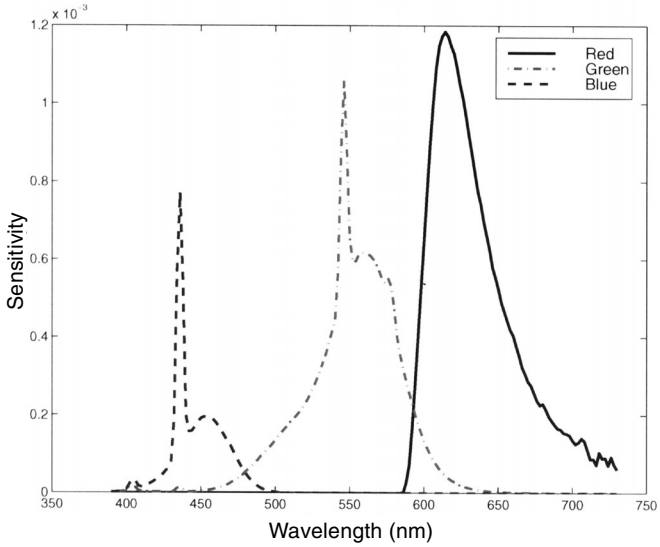

Figure 4. Sensitivities for the simulated scanner channels.

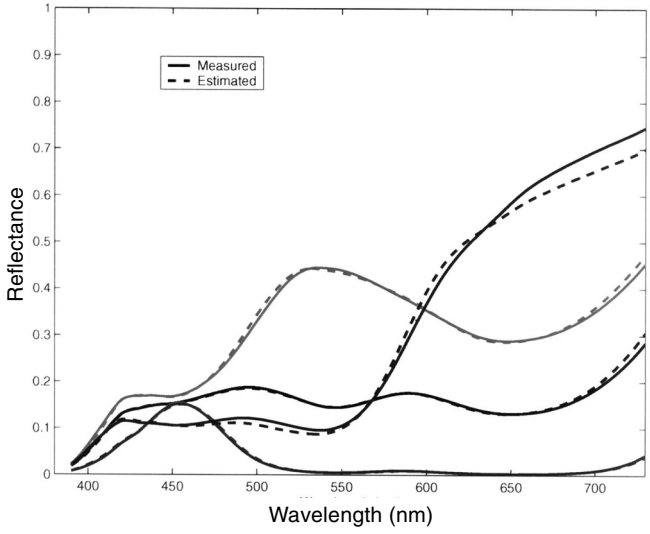

Figure 5. Representative results for the simulated scanner calibration.

Experimental Results

The model-based spectral scanner calibration was also tested on an actual three channel UMAX color scanner with 10 bits per channel. Because the scanner spectral sensitivities for the red, green, and blue channels were not directly available, these were first estimated by the principal eigenvector technique described in Ref. 16 (information on the internal scanner matrixing was not available and therefore the POCS technique described

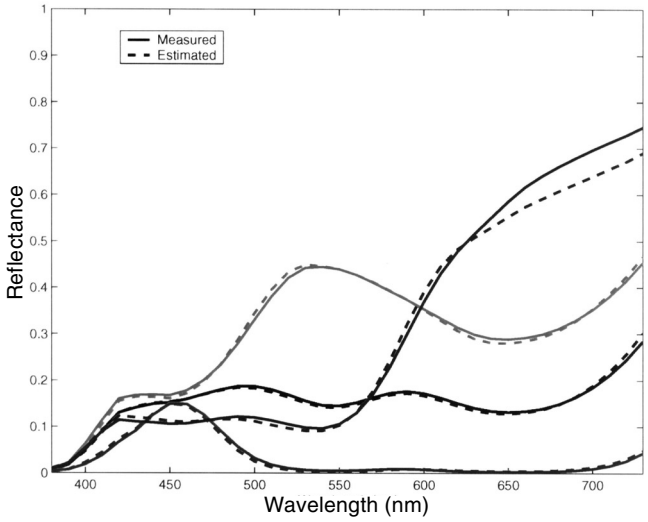

Figure 6. Representative results for the UMAX scanner calibration.

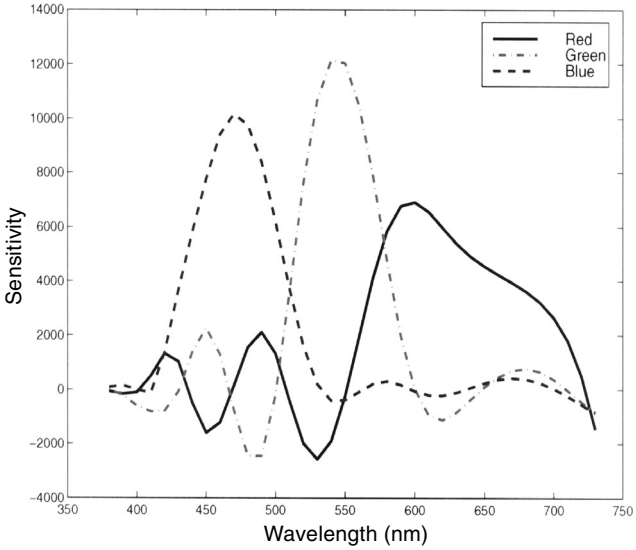

Figure 7. Estimated sensitivities for the UMAX scanner.

in Ref. 16 could not be employed). The estimated sensitivities obtained are shown in Fig. 7.

The Kodak IT8 target was used to evaluate the accuracy of the model based calibration. The model for the medium was obtained as described earlier in the **Practical Implementation Section**. The scanner was used to acquire an RGB image of the target and the average RGB value corresponding to each of the color patches on the target was computed. These scanner RGB values were used along with the scanner and media models in the model-based calibration method presented in Table I. Figure 6 illustrates some of the typical results obtained from this procedure. The solid lines in the figure represent the actual measured reflectance corresponding to Kodak IT8 patches and the broken line closest to each of the solid lines represents the corresponding estimate obtained by the model-based calibration procedure. As in the simulated example, the errors in the spectral estimates are quite small.

The same three-error metrics that were used in the simulation was employed for evaluating the calibration accuracy. For the model-based calibration for the UMAX scanner, over the Kodak IT8 target, the NMSSE was –31.03 dB and the average and maximum ΔE^*_{ab} errors were 1.76 and 7.15, respectively. The average and maximum values for the ΔE^*_{94} metric were 1.11 and 5.70, respectively. For comparison, the scanner was also calibrated directly using a neural network based technique[24] with the complete Kodak IT8 as the training set. The average and maximum ΔE^*_{ab} errors (over the Kodak IT8 target) for the direct calibration were 1.05 and 4.40, respectively. While the errors in the model-based calibration are slightly larger than those for the direct calibration, the model-based calibration provides a complete spectral calibration and also a means for calibration when is no target is available for the scanned medium.

The errors in the model-based calibration of the UMAX scanner are slightly larger than those obtained in the simulations of the **Simulation Results Section**. Estimation error in the scanner spectral sensitivities, scanner noise, and deviations from the scanner model of Eq. 6 due to fluorescence, stray light and other nonlinear effects[25,26] are potential causes for the larger errors. An inspection of Fig. 7 shows that the estimated sensitivities for the UMAX scanner have a number of negative and positive lobes that are highly improbable in the actual scanner. With improved estimates of the scanner spectral sensitivity, one would expect improvement in the accuracy of the model-based calibration. A small component of the error in both the simulation and the actual calibration can also be attributed to deviations from the Beer–Bouger media model of Eq. 3.

Conclusions

The model-based scanner calibration scheme presented in this article provides a method for spectral calibration of a scanner for photographic input media without the use of a calibration target. Simulation and experimental results indicate that good accuracy can be obtained for both spectral and colorimetric calibration with the presented technique.

The model-based calibration scheme can be readily generalized for use in several other applications. In particular, the model-based calibration framework can be used to obtain spectrophotometric data for photographic media from densitometers, colorimeters, and digital color cameras, which can also be represented by the model in Eq. 6.

References

1. G. Sharma, Targetless scanner color calibration, in *Proc. IS&T/SID Seventh Color Imaging Conference: Color Science, Systems and Applications*, IS&T, Springfield, VA, 1999, pp. 69–74.
2. R. Luther, Aus Dem Gebiet der Farbreizmetrik, *Z. Tech. Phys.* **8,** 540–558 (1927).
3. H. E. Ives, The transformation of color-mixture equations from one system to another, *J. Franklin Inst.* **16,** 673–701 (1915).
4. B. K. P. Horn, Exact reproduction of color images, *Comp. Vis., Graphics and Image Proc.* **26,** 135–167 (1984).
5. J. J. Gordon and R. A. Holub, On the use of linear transformations for scanner calibration, *Color Res. Appl.* **18**(3), 218–219, (1993).
6. G. Sharma and H. J. Trussell, Digital color imaging, *IEEE Trans. Image Proc.* **6**(7), 901–932 (1997).
7. G. Sharma, S. Wang, D. Sidavanahalli, and K. T. Knox, The impact of UCR on scanner calibration, in *Final Prog. and Proc. IS&T's PICS Conference*, 1998, pp. 121–124, IS&T, Springfield, VA.
8. H. R. Kang, Color Technology for Electronic Imaging Devices, *SPIE*, Bellingham, WA, 1997.

9. M. Nier and M. E. Courtot, Eds., Standards for electronic imaging systems, **CR37,** *SPIE*, Bellingham, WA, 1991.
10. F. Grum and C. J. Bartleson, Eds., *Optical Radiation Measurements: Color Measurement,* vol. 2., Academic Press, New York, 1983, Chap. 7.
11. R. Patterson, Gamma correction and tone reproduction in scanned photographic images, *SMPTE Journal* **103,** 377–385 (1994).
12. P. L. Combettes, The foundations of set theoretic estimation, *Proc. IEEE* **81**(2), 182–208 (1993).
13. A. Friedman, *The Foundations of Modern Analysis,* Dover, New York, 1982.
14. P. L. Combettes, Generalized convex set theoretic image recovery, in *Proc. IEEE Intl. Conf. Image Proc.* vol. II, 1996, pp. 453–456.
15. G. Sharma, Set theoretic estimation for problems in subtractive color, to appear in *Col. Res. Appl.* **25**(4) (2000).
16. G. Sharma and H. J. Trussell, Set theoretic estimation in color scanner characterization, *J. Electronic Imaging* **5**(4), 479–489 (1996).
17. I. T. Jolliffe, *Principal Components* Analysis, Springer–Verlag, Berlin, 1986.
18. J. A. S. Viggiano and C. J. Wang, A novel method for colorimetric calibration of color digitizing scanners, *Proc. TAGA*, 143–160 (1993).
19. R. S. Berns and M. J. Shyu, Colorimetric characterization of a desktop drum scanner using a spectral model, *J. Electronic Imaging* **4**(4), 360–372 (1995).
20. M. A. Rodriguez and T. G. Stockham, Producing colorimetric data from densitometric scans, *Proc. SPIE Human vision, visual processing, and digital display IV,* **1913,** 413–418 (1993).
21. Kodak Filters for Scientific and Technical Uses, Eastman Kodak Company, Rochester, NY, 1985, Kodak Pub. B-3, (ISBN 0-87985-282-8), CAT 152 8108.
22. CIE, Colorimetry, CIE Publication No. 15.2, Central Bureau of the CIE, Vienna, 1986.
23. CIE, Industrial color difference evaluation, CIE Publication No. 116-1995, Central Bureau of the CIE, Vienna, 1995.
24. H. R. Kang, Color scanner calibration, *J. Imaging Sci. Technol.* **36**(2), 162–170 (1992).
25. J. E. Farrell and B. A. Wandell, Scanner linearity, *J. Electronic Imaging* **2**(3), 225–230 (1993).
26. K. T. Knox, Integrating cavity effect in scanners, in *Proc. IS&T/OSA Optics and Imaging in the Information Age,* IS&T, Springfield, VA, 1996, pp. 83–86.